

DESY SR 84-02  
January 1984

Eigentum der Property of	DESY	Bibliothek library
Zugang: Accessions:	- 1. MRZ. 1984	
Leihfrist: Loan period:	7	Tage days

SURFACE SEGREGATION AND MIXED VALENCY IN DILUTE  
Yb-A1 INTERDIFFUSION COMPOUNDS

by

Ralf Nyholm

*Institute of Physics, Uppsala University, Sweden*

Ib. Chorkendorff

*Institute of Physics, Odense University, Denmark*

Jens Schmidt-May

*II. Institut f. Experimentalphysik, Universität Hamburg*

ISSN 0723-7979

NOTKESTRASSE 85 · 2 HAMBURG 52

DESY behält sich alle Rechte für den Fall der Schutzrechtserteilung und für die wirtschaftliche Verwertung der in diesem Bericht enthaltenen Informationen vor.

DESY reserves all rights for commercial use of information included in this report, especially in case of filing application for or grant of patents.

To be sure that your preprints are promptly included in the  
HIGH ENERGY PHYSICS INDEX ,  
send them to the following address ( if possible by air mail ) :

DESY  
Bibliothek  
Notkestrasse 85  
2 Hamburg 52  
Germany

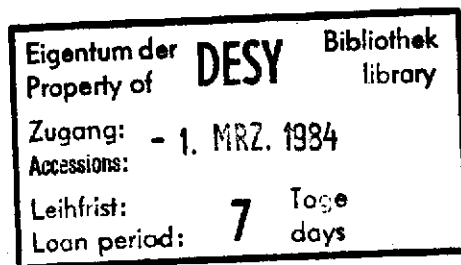
SURFACE SEGREGATION AND MIXED VALENCY IN  
DILUTE Yb-Al INTERDIFFUSION COMPOUNDS

Ralf Nyholm<sup>a)</sup>, Ib Chorkendorff<sup>b)</sup>, Jens Schmidt-May<sup>c)</sup>  
HASYLAB, Hamburg, Germany

- a) Institute of Physics, Uppsala University, P.O. Box 530,  
S-751 21 Uppsala, Sweden
- b) Institute of Physics, Odense University, DK-5230 Odense,  
Denmark
- c) II. Institut für Experimentalphysik, Universität Hamburg,  
D-2000 Hamburg 50, Germany

Abstract

Photoemission experiments on mixed valent Yb-Al compounds prepared by diffusing Yb into an Al (110) single crystal are reported. At high Yb concentrations surface core level peaks reveal a purely divalent surface in agreement with recent results for single crystal YbAl<sub>2</sub>. In the dilute limit, when the intensity from bulk Yb is reduced below the limit of detection, a surface layer of divalent Yb still persists and a surface segregation of Yb in Al is made evident. When the bulk concentration of Yb is reduced the bulk mean valence increases. For diluted samples, when the formation of YbAl<sub>3</sub> in a surrounding of elemental Al is expected, Yb is still in a mixed valent state. The highly resolved structures from trivalent Yb are compared with a recent calculation of the 4f<sup>13</sup> → 4f<sup>12</sup> multiplet pattern.



PACS: 79.60

## 1. Introduction.

Yb-Al intermetallic compounds have been subject to considerable interest due to their mixed valence behaviour. Ytterbium which in its metallic state is divalent with a filled 4f level is found in both divalent ( $f^{14}$ ) and trivalent ( $f^{13}$ ) states in Yb-Al.

The mixed valence character of Yb in Al is of the homogeneous type, i.e. the valence fluctuates between the divalent and trivalent configurations (see e.g. ref. 1).

Photoemission has proved to be a valuable tool for the investigation of the electronic properties of mixed valence compounds. Especially accessible are mixed valence systems involving rare-earth metals. This is due to their unfilled and localized 4f orbitals. A photoemission spectrum of the 4f level shows a multiplet structure characteristic of the initial occupation number. The 4f multiplet structures from different initial occupancies are generally separated in binding energy which facilitates the detection of a mixed valent behaviour. Also the mean valence can be determined from the relative intensities of the multiplet structures. However, recent photoemission studies of several mixed-valent rare-earth compounds have shown that the surface is divalent in contrast to the mixed valent bulk.<sup>2-6</sup> The preference of a divalent state at the surface can be understood from the decrease in cohesive energy due to the reduced coordination for a surface atom. This means that the surface core levels will shift to higher binding energies with respect to the bulk core levels<sup>7</sup> whereby the divalent configuration will be stabilized. In order to accurately determine the bulk mean valence, the experiment must be performed

with a resolution high enough to distinguish between the surface and bulk structures. In the case of Yb this experimental requirement can be fulfilled since in the divalent state the Yb 4f level is filled and the photoemission spectrum shows the spin-orbit split  $4f^{13}$  final states with a large surface to bulk binding energy shift. Trivalent Yb, however, has a 4f spectrum with several multiplets corresponding to the  $4f^{13} \rightarrow 4f^{12}$  transition.

Several electron spectroscopic studies of the Yb-Al system have been made for  $\text{YbAl}_2$ <sup>3</sup>,  $\text{YbAl}_3$ <sup>8,9</sup>, and interdiffusion compounds.<sup>10,11</sup> In this paper we report results from dilute Yb-Al interdiffusion compounds with emphasis on the surface structure and the bulk mean valence. In measurements on single crystal  $\text{YbAl}_2$  it was found that the two topmost surface layers were divalent.<sup>3</sup> These surface layers manifest themselves by showing two different peaks. We find similar surface structures in the compounds with high Yb concentration and are able to follow these structures through the diffusion process. In the dilute limit Yb is found only at the surface and a surface segregation of Yb in Al is evident. The bulk mean valence is seen to increase from 2.4 to about 2.7 as the Yb concentration is lowered. Due to the ability of Yb and Al to form intermetallic compounds we expect to find  $\text{YbAl}_3$  in a surrounding of elemental Al at low Yb concentrations.<sup>12</sup> The present results show that Yb is still in a mixed valent state even at a mean bulk concentration of only a few atomic percent.

## 2. Experimental.

The experiments were performed at the Hamburger Synchrotronstrahlungslabor HASYLAB, with the FLIPPER monochromator.<sup>13</sup> The photoelectrons were analyzed in a commercial double pass CMA. Details of the experimental set-up are given in ref. 14. The instrumental resolution, including the monochromator, was 0.24 - 0.45 eV in all spectra reported here. The higher resolution was used in most of the  $h\nu = 40$  eV and  $h\nu = 100$  eV spectra when detailed information on the Yb 4f structures was sought, whereas the lower resolution was used in the spectra recorded at higher photon energies ( $h\nu = 170-190$  eV).

## 3. Preparation of Mixed Valent Samples.

The samples were prepared by evaporating a thin layer (50Å) of Yb onto an Al (110) single crystal, which had been cleaned by Ar<sup>+</sup> ion sputtering and was subsequently annealed. During the initial stage of the diffusion of Yb into the Al crystal the spectra in Figure 1 were recorded and the Yb 4f<sub>7/2,5/2</sub> bulk peaks (at binding energies 1.2 eV and 2.4 eV in the pure metal) were found to shift continuously towards the Fermi edge. Also the 4f peaks from surface atoms, shifted to higher binding energies, were seen to move closer to the Fermi edge. It should be noted that spectrum 1b, recorded immediately after evaporation, shows that a reaction between the Yb and Al has already taken place. Short heat treatments (typically 5 min. at about 800 K) and subsequent cooling to room temperature were made to produce the samples yielding the spectra shown in Figures 1c and 1d. A spectrum from the latter sample, recorded at higher photon energy, is shown

over a wider energy range in Figure 2a and reveals 4f structures typical of mixed valent Yb. Close to the Fermi level we see the two overlapping 4f<sup>14</sup> → 4f<sup>13</sup> spin-orbit doublets from Fig. 1d and between 5 and 10 eV binding energy the multiplets of the 4f<sup>13</sup> → 4f<sup>12</sup> transition of trivalent Yb. The observation of emission from both divalent and trivalent Yb together with the appearance of the bulk divalent 4f peak close to the Fermi level (binding energy 0.15±0.05 eV) is a necessary requirement for a homogeneous mixed-valent compound.<sup>1</sup> The overall structure of the spectrum in Fig. 2a resembles the spectrum of single crystal YbAl<sub>2</sub> from ref. 3.

In order to investigate Yb-Al compounds of even lower Yb concentration, the heat treatments were repeated several times yielding the spectra b,c and d in Fig. 2. After each heat treatment the sample was cooled to room temperature before recording the spectra and since the diffusion of Yb in Al is very slow at room temperature<sup>11</sup> no changes of the spectra are expected to occur during the measurements. Each heat treatment makes the Yb diffuse further into the Al substrate which is recognized by a substantial decrease in the bulk 4f intensity (see Fig. 2a to 2d).

## 4. Results and discussion.

### 4.1 Surface segregation.

Ultimately the diffusion is driven so far that the bulk 4f intensity totally vanishes. This is the situation met with in spectrum 2d where only the Yb 4f surface peaks and the Al valence band are seen. As is evidenced by a comparison between the

different spectra in Fig. 2 and the results of a curve fitting procedure, which will be discussed below, the Yb 4f emission in spectrum 2d corresponds only to a top surface layer of Yb on the Al crystal. Thus this spectrum shows that in the dilute limit Yb still remains at the surface and, furthermore, this Yb is purely divalent. When the sample yielding the spectrum in Fig. 2d is sputtered the Yb 4f peaks disappear and only the valence band spectrum of Al is seen. After annealing, however, the Yb 4f signal reappears and the spectrum looks exactly as before sputtering. This demonstrates that there is a segregation of Yb to the surface of the Al crystal.

This experimental finding can be compared with the prediction of a semi-empirical model by Miedema<sup>15</sup> for surface segregation in binary systems. In this model three energy terms contribute to a difference in surface vis-à-vis bulk composition: (i) the heat of solution of one metal into the other, (ii) the difference in surface energies of the pure constituents, and (iii) an energy associated with the difference in atomic sizes. Due to the low surface energy of Yb (510 mJ/m<sup>2</sup>, calculated from ref. 16) as compared to Al (1200 mJ/m<sup>2</sup>)<sup>16</sup> the second term will be dominating and the model predicts a segregation of Yb to the surface.

#### 4.2 The divalent Yb 4f spectrum.

In order to resolve the surface and bulk peaks we employed a curve fitting procedure using Doniach-Šunjić line shapes<sup>17</sup> for the individual peaks. An inelastic background proportional to the integrated area of the bulk peaks was used. We also added to the fits a signal proportional to the valence band spectrum of pure Al to account for the valence band intensity, which in the

diluted cases (spectra 2c and 2d) gives a considerable contribution to the spectra. In spectrum 2d the surface structures are very symmetric and we used a single 4f spin-orbit doublet with a dominant Gaussian broadening in our fit. The surface structures in spectrum 2a show an asymmetry towards lower binding energies which to some extent is also seen in spectra 2b and 2c. In the fitting procedure we used two spin-orbit doublets to reproduce these surface peaks. For best fits the widths of these peaks are very similar to the widths found for the surface peaks in spectrum 2d. Some of the results from the curve fitting are shown in Figure 3. The set of line parameters used in all fits are given in Table 1 and measured intensity ratios are given in Table 2.

We observe a significantly lower life time width for the bulk 4f<sup>13</sup> peaks (0.06 eV) compared to the 4f<sup>12</sup> multiplets (0.20 eV) and also compared to pure Yb (0.10 eV). The widths of the surface peaks largely exceed the widths of the bulk peaks and the line shapes are best described by a Gaussian distribution. This is most clearly seen in spectrum 2d where no interference from bulk peaks occurs. This broadening is most likely due to different sites for the Yb surface atoms resulting in a distribution of surface shifts.

The shifts of the two surface peaks in spectrum 2a are  $+0.38 \pm 0.05$  eV and  $+0.83 \pm 0.05$  eV with respect to the bulk peak. A slight increase in these surface shifts (about 0.10 eV) is observed in spectra 2b and 2c. The separation of the surface derived structure into two peaks is in agreement with the results for single crystal YbAl<sub>2</sub> reported by Kaindl et.al.<sup>3</sup> who also

interpreted the low binding energy surface peak as emission from a second surface layer. Following this second layer peak through spectra 2a to 2d, we find that it gradually decreases in intensity until it has totally vanished in the dilute limit (see Table 2). This indicates that during the diffusion process the subsurface region is depleted of Yb whereby in the dilute limit Yb is present only at the surface.

#### 4.3 The trivalent Yb 4f spectrum.

So far we have discussed the divalent part of the Yb 4f spectrum. Let us now turn to the trivalent structures. In Figure 4 we show spectra recorded at different photon energies including the  $4d \rightarrow 4f$  resonance region. This resonance, which is due to the interference between the direct photo ionization of a 4f electron and the direct recombination of the excited  $4d^9 4f^{14}$  state, was first observed in the trivalent Yb oxide.<sup>18</sup> At resonance the total 4f emission is enhanced and also the relative intensities between different multiplets change. The spectra in Fig. 4 show the same resonance behaviour as found in the oxide.<sup>18,19</sup> An interesting difference between the  $4f^{13} \rightarrow 4f^{12}$  emission from Yb oxide and that of the Yb-Al compound is the much narrower line widths in the latter case. Thus, we are able to perform a detailed comparison between the measured spectrum and a recent calculation of the multiplet structure of the  $4f^{13} \rightarrow 4f^{12}$  transition made by Gerken.<sup>20</sup> This comparison is shown in Fig. 4 for the spectrum recorded at 100 eV photon energy. Each multiplet has been replaced by a Doniach-Šunjić line shape using the line parameters given in Table 1 with relative positions and intensities from the calculation in ref. 20. As seen in Fig. 4 the agreement between calculation and experiment is very good. All structures

in the spectrum are accounted for by the calculated multiplets. Only a slight intensity difference at binding energies 6 to 8 eV is observed. This is most probably due to intrinsic and/or extrinsic energy losses from the divalent 4f peaks.<sup>11</sup> To some extent these losses have been included in the fit by subtracting the background intensity of the spectrum in Fig. 2d.

#### 4.4 Mixed valency.

Using the results from the line fits for the different parts of the Yb 4f spectra we can estimate the intensity ratios between the trivalent and divalent emission from the bulk (see Table 2) and hence calculate the mean valence of Yb. The measured intensity ratios between the trivalent and divalent peaks ( $I^{12}/I^{13}$ ) are  $0.6 \pm 0.1$ ,  $1.8 \pm 0.4$ ,  $2.6 \pm 1$  in spectra 2a, 2b, and 2c respectively. The big uncertainty for the last spectrum is due to the overlap between the weak bulk divalent peaks and the valence band emission. The mean valence, given by  $2 + I^{12}/(I^{12} + I^{13})$ , is 2.4, 2.6, and 2.7 respectively. This can be compared with the result for  $\text{YbAl}_2$ <sup>3</sup> which was 2.4 in agreement with the value derived from lattice constant measurements.<sup>21</sup> For  $\text{YbAl}_3$  mean valencies of 2.7<sup>22</sup> and 2.95<sup>23</sup> have been reported.

To find the compositions of the samples investigated we have estimated the mean bulk concentration of Yb by comparing the bulk 4f intensities from the Yb-Al samples with the corresponding intensity from pure Yb measured under the same experimental conditions. For the sample yielding spectrum 2a the mean concentration roughly corresponds to  $\text{YbAl}_2$  while in spectra 2b and 2c the concentration is reduced by a factor of 3 and 10 respectively. This estimate, of course, only applies to a shallow region of the crystal due to the small mean free

path of the photoelectrons. Although the above procedure is subject to some uncertainty and should only be considered as a rough estimate, we can safely conclude that the spectrum in Fig. 2c corresponds to an Yb concentration far below that of a homogeneous  $\text{YbAl}_3$  compound. For the Yb-Al system two intermetallic compounds exist:  $\text{YbAl}_2$  and  $\text{YbAl}_3$ .<sup>12</sup> According to the phase diagram<sup>12</sup> these compounds are formed even at non-stoichiometric compositions so that, depending on the concentration, the system consists of: (i)  $\text{YbAl}_2$  in a surrounding of pure Yb (>33 at.% Yb), (ii) a mixture of  $\text{YbAl}_2$  and  $\text{YbAl}_3$  (25 to 33 at.% Yb), or (iii)  $\text{YbAl}_3$  in a surrounding of pure Al (<25 at.% Yb). Thus, the presence of both divalent and trivalent bulk structures in spectrum 2c shows that when  $\text{YbAl}_3$  is diluted in an Al matrix, Yb is still in a mixed valent state. This means that the mixed valence character is determined by the local environment of the Yb atom and is not a property of the whole lattice. A similar behaviour has been found also for Tm in  $\text{Tm}_x\text{Y}_{1-x}$ Se compounds.<sup>6</sup>

## 5. Summary.

In summary, a thin layer of Yb deposited onto an Al (110) single crystal was diffused into the substrate by repeated heat treatments yielding intermetallic mixed valence compounds of different bulk Yb concentrations. It is found that Yb persists in a divalent state at the surface independent of the concentration. The observation of a divalent surface is in agreement with the results for  $\text{YbAl}_2$ .<sup>3</sup> After several heat treatments the bulk Yb concentration is reduced below the limit of detection but the surface signal is still present. When this sample is sputtered the Yb signal disappears but is completely restored by annealing.

This shows that there is a segregation of Yb to the Al surface. By comparing the intensities for the trivalent and divalent Yb bulk signals it is also found that the mean valence increases as the Yb concentration is decreased. It is concluded that  $\text{YbAl}_3$  in a surrounding of pure Al still retains its mixed valence character which points towards a local description of homogeneous mixed valency.

## Acknowledgements

This work was supported by the Swedish Natural Science Research Council, the Danish Natural Science Research Council and the Bundesministerium für Forschung und Technologie.



References.

1. M. Campagna, G.K. Wertheim and F. Bucher, *Struct. Bonding* 30, 99 (1976).
2. V. Murgai, L.C. Gupta, R.D. Parks, N. Mårtensson and B. Reihl, in *Valence Instabilities*, Eds. P. Wachter and H. Boppart, North-Holland, Amsterdam (1982), p.299.
3. G. Kaindl, B. Reihl, D.F. Fastman, R.A. Pollak, N. Mårtensson, B. Barbara, I. Penney and T.S. Plaskett, *Sol. Stat. Commun.* 41, 157 (1982).
4. N. Mårtensson, B. Reihl, W.D. Schneider, V. Murgai, L.C. Gupta and R.D. Parks, *Phys. Rev. B* 25, 1446 (1982).
5. G. Kaindl, C. Laubschat, B. Reihl, R.A. Pollak, N. Mårtensson, F. Holtzberg and D.E. Eastman, *Phys. Rev. B* 26, 1713 (1982).
6. N. Mårtensson, B. Reihl, R.A. Pollak, F. Holtzberg, G. Kaindl and D.F. Fastman, *Phys. Rev. B* 26, 648 (1982).
7. B. Johansson, *Phys. Rev. B* 19, 6615 (1979).
8. K.H.J. Buschow, M. Campagna and G.K. Wertheim, *Sol. Stat. Commun.* 24, 253 (1977).
9. W.F. Egelhoff, Jr. and G.G. Tibbets, *Phys. Rev. Lett.* 44, 482 (1980).
10. G.G. Tibbets and W.F. Egelhoff, Jr., *J. Vac. Sci. Technol.* 17, 458 (1980).
11. J. Onsgaard, I. Chorkenderff, D. Ellegaard and U. Sørensen, to be published.
12. A. Palenzona, *J. Less Common Met.* 29, 289 (1972).
13. J. Barth, F. Gerken, C. Kunz and J. Schmidt-May, *Nucl. Instr. and Methods* 208, 307 (1983).
14. J. Barth, F. Gerken and C. Kunz, *Nucl. Instr. and Methods* 208, 797 (1983).
15. A.R. Miedema, *Z. Metallkde.* 69, 455 (1978).
16. A.R. Miedema, *Z. Metallkde.* 69, 287 (1978).
17. S. Doniach and M. Šunjić, *J. Phys. C* 3, 285 (1970).
18. L.I. Johansson, J.W. Allen, T. Lindau, M.H. Hecht and S.B. Hagström, *Phys. Rev. B* 21, 1408 (1980).
19. J. Schmidt-May, R. Nyholm, F. Gerken and L.C. Davis, to be published.
20. F. Gerken, *J. Phys. F* 13, 703 (1983).
21. I. Penney, B. Barbara, R.L. Melcher, T.S. Plaskett, H.E.

King, Jr. and S.J. La Placa, in Valence Fluctuations in Solids, Eds. M.L. Falicov, W. Hanke and M.B. Maple, North-Holland, Amsterdam (1981).

22. B.C. Sales and D.K. Wuhlleben, Phys. Rev. Lett. 35, 1240 (1975).

23. R.E. Majewski, A.S. Edelstein, A.T. Aldred and A.E. Dwight, J. Appl. Phys. 49, 2096 (1978).

TABLE 1

Parameters used in the line fits of the spectra in Figure 2. The line widths are given as full-widths at half-maximum. The 1st surface peak corresponds to the high binding energy component.

	Life time width (eV)	Asymmetry	Gaussian broadening (eV)
Bulk $f^{13}$	0.06	0.10	0
Bulk $f^{12}$	0.20	0.10	0
1st surface peak	0.20	0.05	0.45
2nd surface peak	0.20	0.10	0.45

TABLE 2

Relative intensities of the different Yb 4f structures for the spectra in Figure 2. Total peak areas were derived from the line fits and normalized to unit area for the 1st surface peaks.

Spectrum	Area relative to 1st surface peak		
	Bulk $f^{13}$	Bulk $f^{12}$	2nd surface
2a	0.59	0.38	0.75
2b	0.21	0.37	0.56
2c	0.04	0.10	0.22
2d	0	0	0

### Figure Captions

Figure 1. The Yb 4f spectrum after evaporation of a thin layer of Yb onto an Al (110) single crystal. The spectra (b), (c) and (d) were recorded during the initial diffusion stage. For comparison a spectrum from pure Yb (a) is also shown.

Figure 2. Electron spectra from Yb-Al interdiffusion compounds showing the bulk and surface derived 4f spin-orbit doublets from divalent Yb at low binding energy and the multiplets from the  $4f^{13} \rightarrow 4f^{12}$  transition in trivalent Yb at binding energies 5 to 10 eV. Spectra (a) to (d) were recorded from samples with decreasing bulk concentrations of Yb. In spectrum (d) the bulk divalent and trivalent structures have been reduced below the limit of detection and only the surface peaks from divalent Yb are seen.

Figure 3. The figures (a), (b) and (c) show line fits for spectra (a), (c) and (d) of fig. 2 respectively. Also shown is a fit for a spectrum recorded at  $h\nu = 40$  eV from the same sample as in spectrum (d) in Fig. 2. Inserted are the individual components of the narrow bulk and broad surface spin-orbit doublets. Also included are the calculated inelastic background and the estimated valence band emission. For the sake of clarity these have been omitted in spectrum (a).

Figure 4. The 4f structures from trivalent Yb recorded at photon

energies passing through the  $4d \rightarrow 4f$  resonance. The individual multiplets of the  $4f^{13} \rightarrow 4f^{12}$  transition show a similar intensity enhancement as found in the trivalent Yb oxide. Also included, as a bar diagram, are the calculated positions and intensities of the  $4f^{13} \rightarrow 4f^{12}$  transition from ref. 20. A curve fit based on this calculation is shown for the spectrum recorded at  $h\nu = 100$  eV. (this spectrum is not on scale with the other spectra).

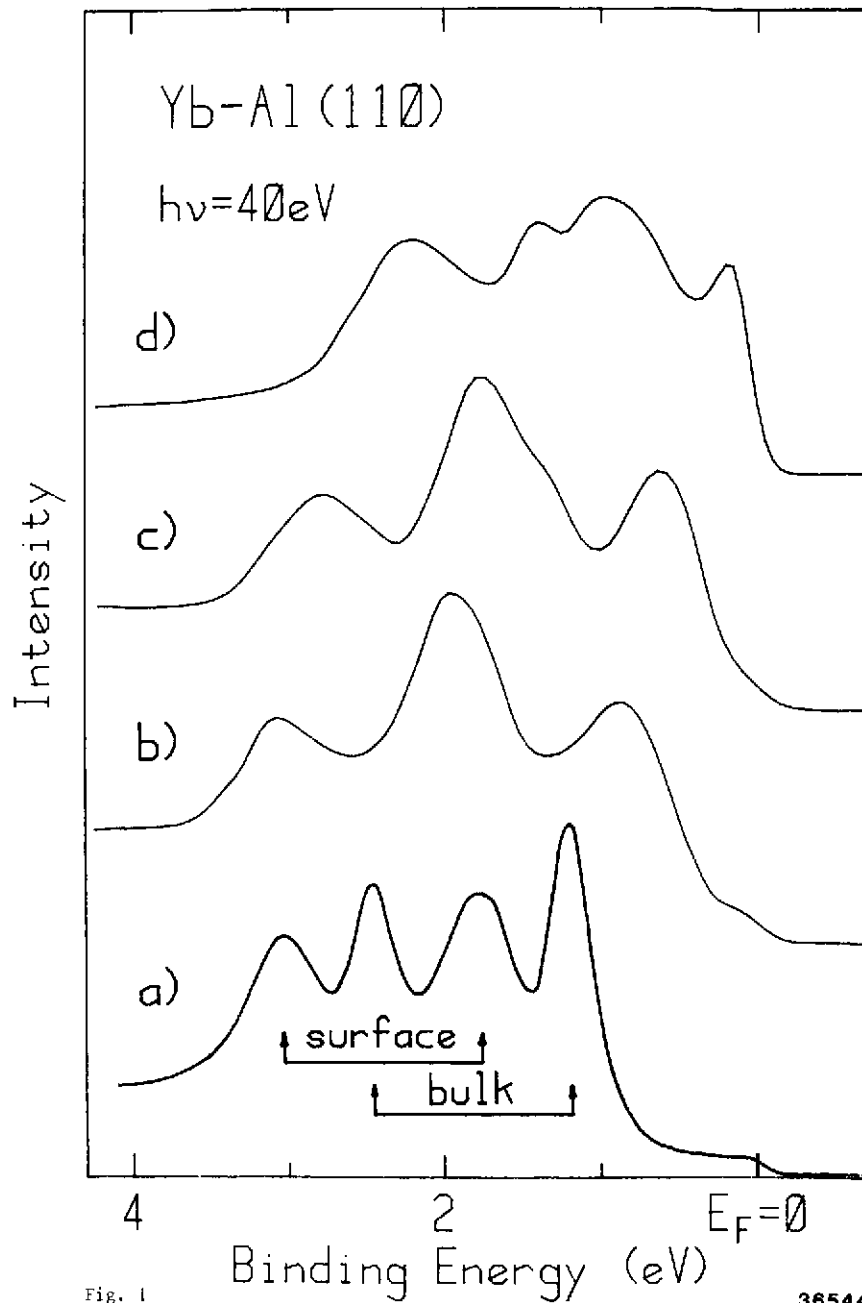


Fig. 1

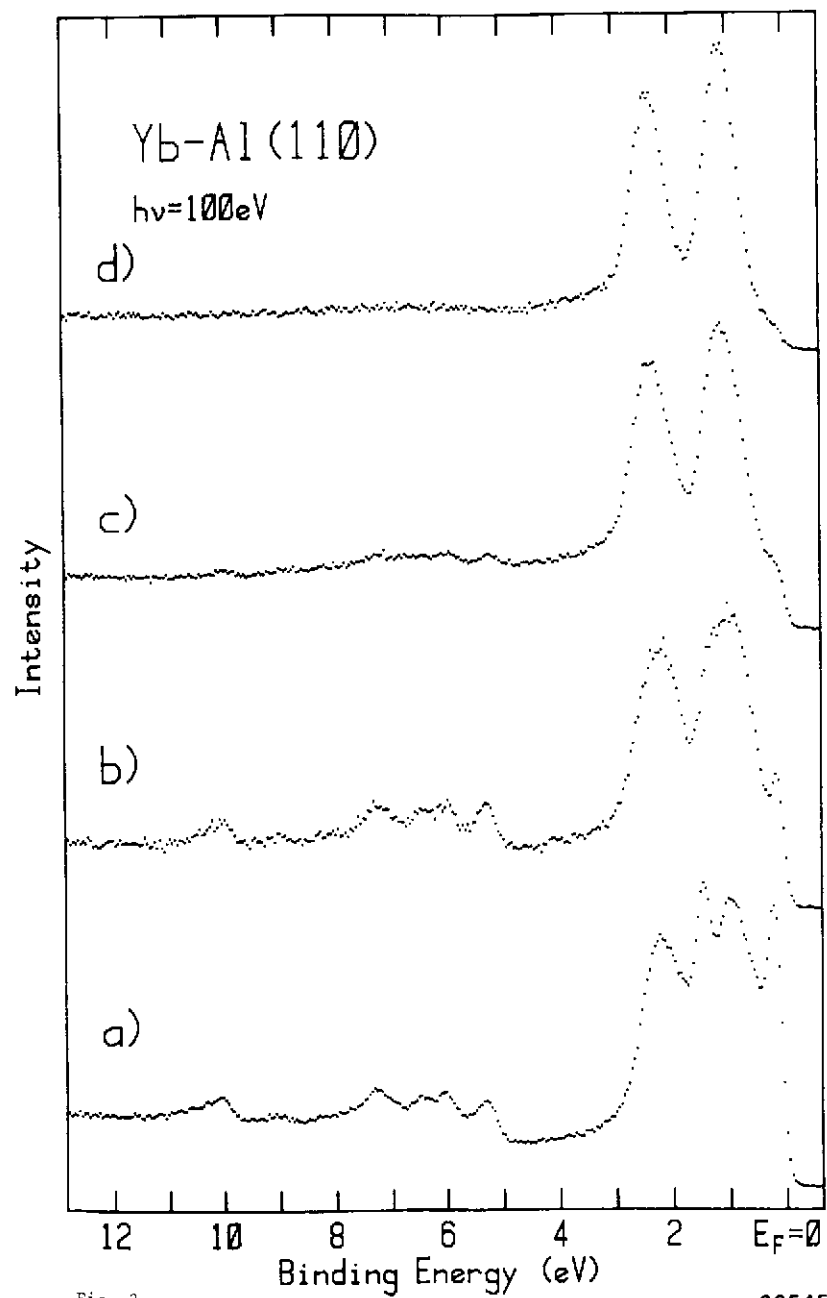


Fig. 2

36545

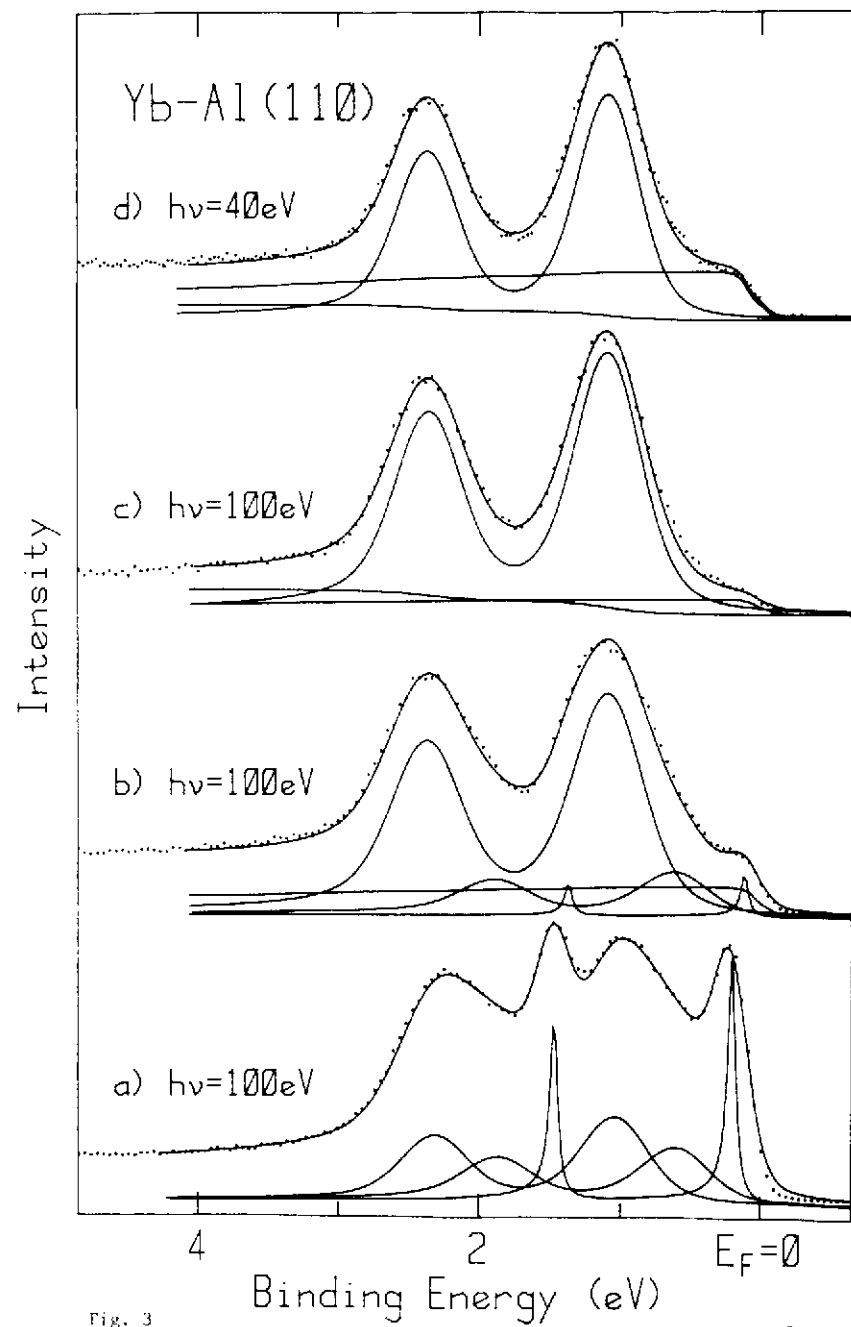


Fig. 3

36543

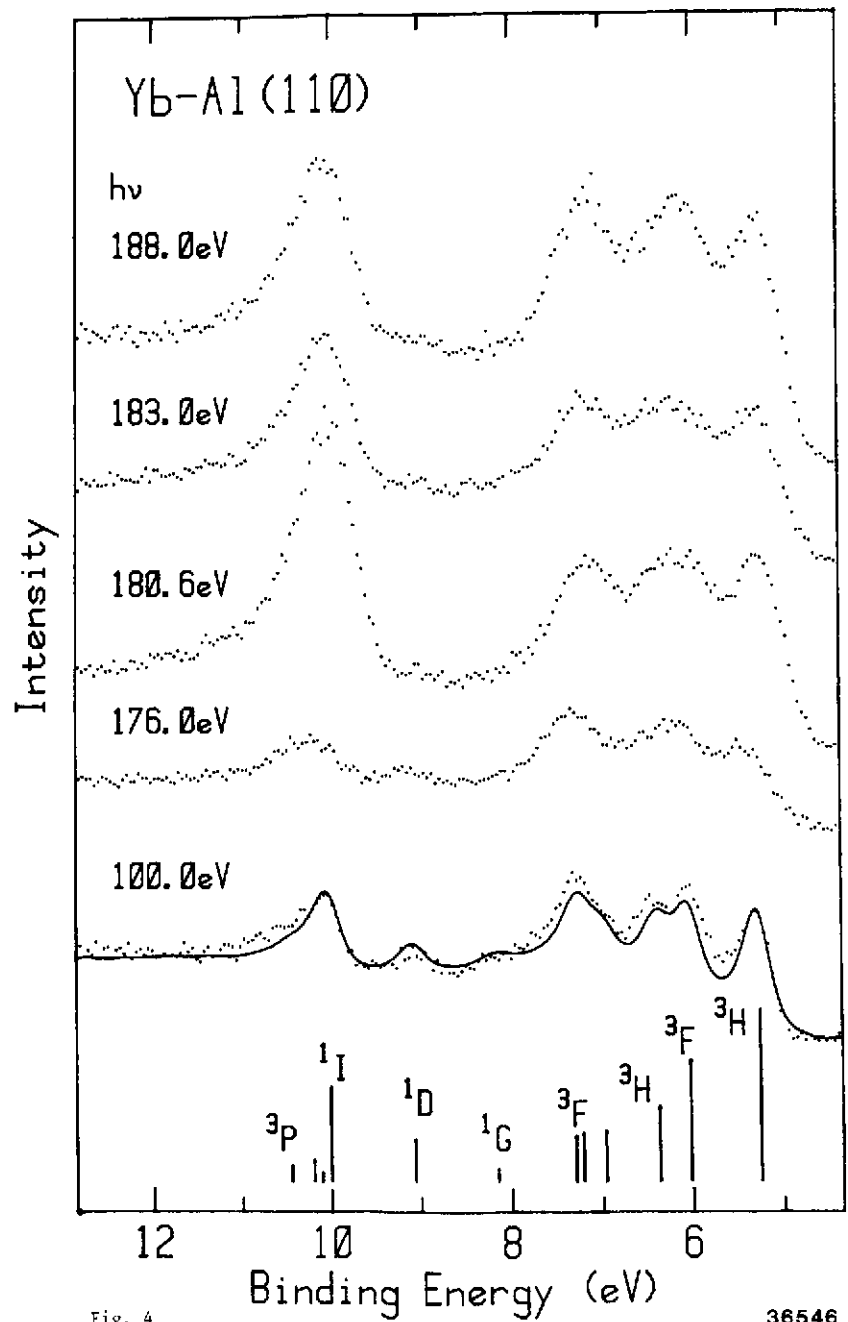


Fig. 4

36546